Effect of Big-Cube Zr_2Ni on the Absorption and Desorption Kinetics of Nanocrystalline MgH_2 Powders

M. Sherif El-Eskandarany, H. Al-Matrouk, Ahmed Al-Duweesh and Ehab Shaban

Nanotechnology and Advanced Materials Program,
Energy and Building Research Center, Kuwait Institute for Scientific Research
Safat 13109, Kuwait - State of Kuwait, msherif@kisr.edu.kw

ABSTRACT

A new hydrogen storage system of nanocomposite MgH_2/10 wt.% big-cube Zr_2Ni nanocrystalline powders were synthesized. A β-MgH_2 phase coexisted with small mole fractions of γ-MgH_2 nanocrystalline ultrafine powders were obtained after reactive ball milling (RBM) technique of pure Mg powders of metallic Mg powders under a pressure of 50 bar of hydrogen gas. Mechanical alloying technique, using a high-energy ball milling was employed to fabricate big-cube phase of Zr_2Ni nanocrystalline powders starting from tetragonal-Zr_2Ni alloy prepared by arc melting technique. The hydrogenation/dehydrogenation properties of nanocomposite MgH_2/10 big-cube Zr_2Ni powders possessed fast sorption and desorption kinetics at 250 ºC. The system absorbed 4.9 wt.% H_2 within 92 s, whereas it released the absorbed hydrogen within 320 s. At 250 ºC, the synthesized nanocomposite system in the present study showed extraordinary high absorption/desorption cycles for any MgH_2 system, as far as the authors know, which reached to 2546 complete cycles covered in 1240 h.

Keywords: reactive ball milling, mechanical alloying, metal hydrides, Zr-based metastable alloys, gas sorption/desorption kinetics, cycle-life-time

1 INTRODUCTION

However, the hydrogenation/dehydrogenation processes (absorption/desorption) kinetics of MgH_2 is very slow, Mg metal with its low cost and high capability to store a high hydrogen content (7.60 wt.%) is considered to be the most promising materials for solid-state hydrogen storage in light vehicles [1]. The absorption and desorption kinetics of MgH_2 powders prepared by RBM process [2] can be improved by subjecting the powders to long-term of milling [3]. Further improvement of can be also achieved by mechanical alloying of MgH_2 with 3d transition metals [4] and their oxides [5].

Although there are many reported efforts performed to improve the hydrogenation/dehydrogenation properties of MgH_2 system [6], there is a still space for new attempts that aims to find a suitable catalytic system used to improve the absorption and desorption kinetics of this promising metal hydride system. The present study was tackled in order to investigate the effect of a new nanocatalyst system (big-Zr_2Ni) used for the first time on improving the hydrogenation and dehydrogenation kinetics of MgH_2 system synthesized by RBM technique.

2 EXPERIMENTAL PROCEDURE

Hydrogen gas (99.999 %), elemental Mg powders (~ 80 μm, 99.8 %), bulk Zr (99.7%) and bulk Ni metals were used in the present study. Small amount of the Mg powders (5 g) was balanced inside a helium (He) gas atmosphere (99.99%) - glove box and then were sealed together with twenty five hardened steel balls into a hardened steel vial (220 ml in volume), using a gas-temperature-monitoring system (GST). The ball-to-powder weight ratio was 40:1. The vial was then evacuated to the level of 10^{-3} bar before introducing H_2 gas to fill the vial with a pressure of 50 bar. The milling process was carried out at room temperature using high energy ball mill operated at a rotation speed of 250 rpm. After 25 h of RBM the powders were discharged from the vial inside the glove box and then mixed with 10 wt.% of previously prepared big-cube-Zr_2Ni nanocrystalline powders [7]. The mixed powders were then ball milled for 50 h, using a high energy ball mill. The structure, morphology, elemental analysis, thermal stability, composition, and the hydrogenation/dehydrogenation kinetics of the all samples obtained after different ball milling time were invistigated. X-ray diffraction (XRD) with CuKα radiation, 200 kV-field emission high resolution transmission electron microscopy/scanning transmission electron microscopy (FE-HRTEM/STEM), equipped with energy-dispersive X-ray spectroscopy (EDS), 15 kV-field emission scanning electron microscope (FE-SEM/EDS), differential scanning calorimetery (DSC), and Sievert's approach were employed to characterize and investigate the different properties of the ball milled powders.

3 RESULTS AND DISCUSSIONS

Figure 1 The XRD patterns of the staring reactant materials of Mg powders is shown in Fig. 1(a). At this initial stage of RBM time, the powders were polycrystalline hcp-Mg phase with large grains, suggested by the sharp diffraction Bragg's peaks shown in Fig. 1(a). After 1 h of the reactive ball milling (RBM) time, a small mole fraction of a new phase could be detected, as suggested by the low

intensity Bragg-peaks denoted by squared symbols in Fig. 1(b). Comparing the Bragg-peak positions of this new phase with those reported for tetragonal β-MgH_2 confirmed the formation of β-MgH_2 phase after this early stage of RBM. After 3 h of RBM time, the mole fraction of the existed β-MgH_2 phase in the milled powders was increased, suggested by the appearance of pronounced and sharp Bragg peaks corresponding to the β-MgH_2 phase, as presented in Fig. 1(c). Whereas, the Bragg's peaks corresponding to the β-MgH_2 phase become very sharp and more pronounced after 6 h of the RBM time (Fig. 1(d)), the Bragg's lines for non-reacted Mg crystals can hardly be seen, implying a continuous increasing in the mole fractions of the formed hydride phase against the unreacted Mg powders, respectively. After 25 h of the RBM time, nanocrystalline β-MgH_2 coexisting with small mole fraction of γ-MgH_2 phases were obtained, suggested by the obvious broadening in the Bragg's lines for both phases, as shown in Fig. 1(e). Low-intensity peaks (less than 40 cps) of cubic-MgO phase, which has a lattice constant of a_o=0.4216 nm, were detected in sample. This oxide phase appeared as a result of surface oxidation of the fine MgH_2 powders during the sample preparations for XRD.

The image of the high resolution transmission electron microscope (HRTEM) for the powders obtained after 25 h of RBM time is presented in Fig. 2. The formation of ultrafine grains, ranging from 4 to 8 nm, of β-MgH_2 and γ-MgH_2 phases can be obviously seen, as denoted by the Miller indexed zones (Fig. 2).

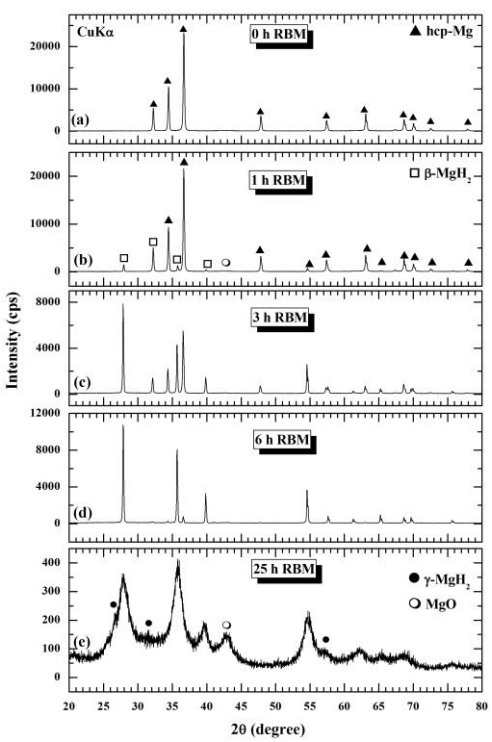

Figure 1: XRD patterns of Mg powders after RBM time for (a) 0 h, (b) 1 h, (c) 3 h, (d) 6 h and (e) 25 h.

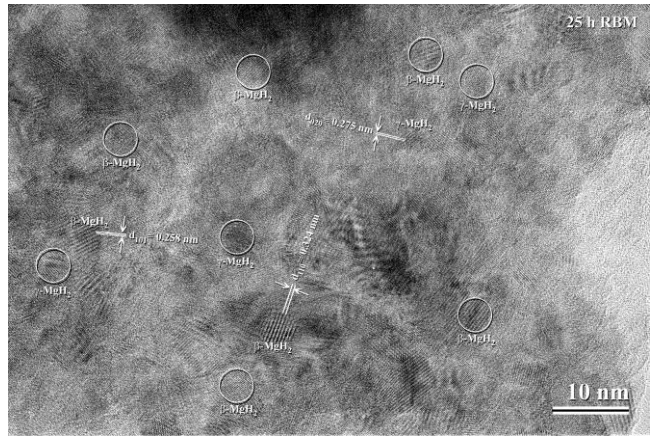

Figure 2: HRTEM image of Mg powders obtained after RBM time for 25 h.

The thermal stability of synthesized MgH_2 powders after different RMB time was investigated by DSC analysis at a constant heating rate of 20 °C/min. The DSC thermograms of the powders obtained after selected RBM times are shown in Fig. 3. The decomposition event for the sample obtained after 6 h of RBM time took place through a single-endothermic peak (Fig. 3(a)), suggesting the existence of a single phase of β-MgH_2. The onset and peak decomposition temperatures were 438 °C and 459 °C, respectively. These temperatures tended to be shifted to the low temperature side after 12.5 h of the RBM time (Fig. 3(b)) and found to be 431 °C (onset temperature) and 451 °C (peak temperature), suggesting a destabilization on the β-MgH_2 phase.

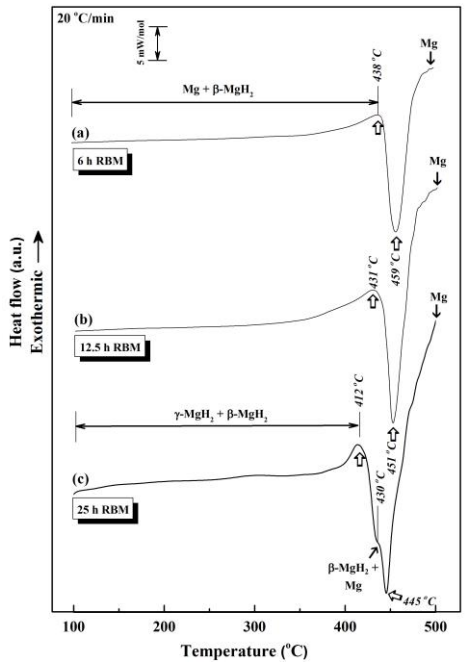

Figure 3: DSC curves of Mg powders obtained after RBM time for (a) 6 h, (b) 12.5 h and (c) 25 h.

The DSC trace for the sample, which was obtained after 25 h of the RBM time revealed a shoulder-like endothermic peak, suggesting two-decomposition stages, as shown in Fig. 3(c). The first decomposition event refers to the decomposition of the γ-MgH_2 into β-MgH_2 and Mg powders, as confirmed by the XRD analysis (not shown here). The first endothermic peak, which characterized by an onset temperature of 412 ^oC, vanished at an end-set temperature of about 430 ^oC, where the second decomposition peak (β-MgH_2 →Mg) starts. The peak temperature of the second decomposition event is recorded and found to be 445 ^oC, suggesting a continuous destabilization of the formed hydride phase, as shown in Fig. 3(c).

According to the poor hydrogenation/dehydrogenation kinetics of as-synthesized MgH_2 powders and in part to propose a new nanocatalyst system, we prepared big-cube Zr_2Ni nanopowders [7] for using as catalysts to improve the kinetic of absorption and desorption of MgH_2 powders and to maximize its cycle-life time. The as-synthesized MgH_2 powders obtained after 25 h of the RBM were mixed with 10 wt.% of the big-cube and then ball milled under hydrogen gas pressure for 50 h. The XRD patterns of the big-cube phase obtained after 150 h of ball milling is shown in Fig. 4(a). Obviously, very broad Bragg peaks were appeared, suggesting the formation of nanocrystalline phase. The analysis of the diffracted lines presented in Fig. 4(a) suggests that the powders at this stage of ball milling reveal polycrystalline structure corresponding to Ti_2Ni [8] structure ($E9_3$ structure, space group Fd3m).

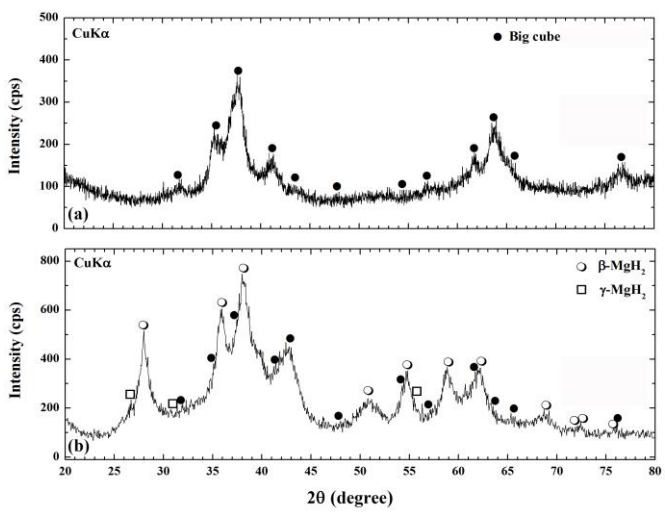

Figure 4: (a) XRD patterns of big-cube Zr_2Ni nanocrystalline powders obtained after 150 h of ball milling time. The XRD pattern of as-prepared MgH_2 powders and then ball milled with the big cube phase for 50 h under a hydrogen gas atmosphere is shown in (b).

The STEM-BFI and of the nanocomposite MgH_2 doped with 10 wt.% Zr_2Ni obtained after 50 h of ball milling is shown in Fig. 5. The light gray matrix shown in the figure is for MgH_2 matrix whereas the spherical dispersoids nanoparticles (~3 – 11 nm in diameter) embedded into the matrix are nano-cells big cube phase.

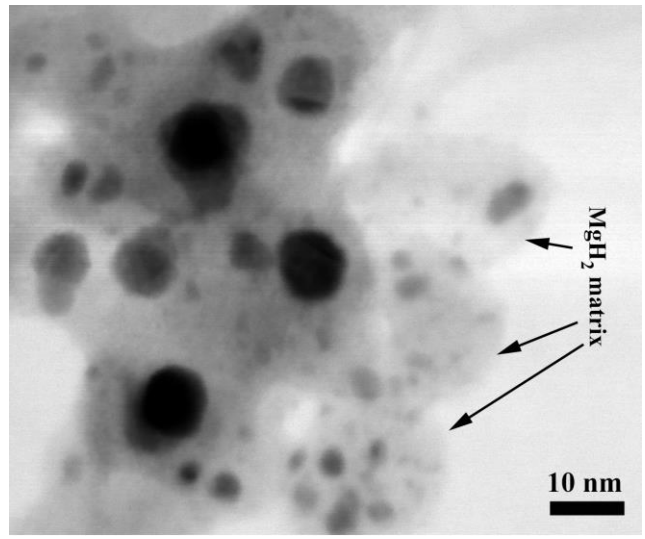

Figure 5: STEM-BFI and of MgH_2/10 Zr_2Ni nanocomposite powders obtained after 50 h of ball milling time.

The DSC analysis was performed in order to investigate the effect of big-cube Zr_2Ni additive on the thermal stability of MgH_2 powders. The DSC trace of the nanocomposite powders obtained after 50 h of the ball milling time is displayed in Fig. 6(a). There are two opposite reactions shown in the micrograph. The first reaction is an endothermic and refers to the decomposition of β-MgH_2 phase into hcp-Mg that taken place at an onset temperature of 288 ^oC, as shown in Fig. 6(a). Comparing this value with that one for pure MgH_2 powders (431 ^oC; Fig. 3(c)) one can be noted that adding the big-cube phase leads to decrease the decomposition temperature of β-MgH_2 phase by a value of 143 ^oC and this indicates a crucial effect of the big-cube phase on destabilizing of the MgH_2 phase. The XRD pattern of the sample heated up to 324 ^oC (just above the endothermic reaction) reveals Bragg-peaks related to hcp-Mg and big-cube Zr_2Ni phase, without any evidence for the formation of any other phases, as displayed in Fig. 6(b).

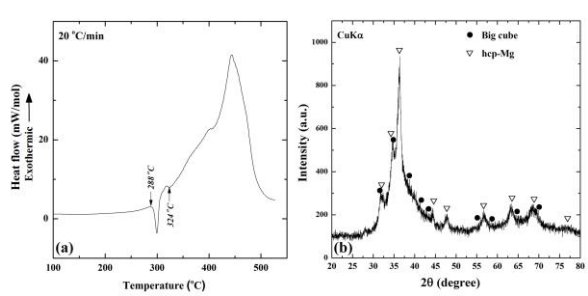

Figure 6: (a) DSC curves of MgH_2 powders obtained after RBM for 25 h and then ball milled with 10 wt.% of big-cube Zr_2Ni for 50 h. The XRD pattern of a sample heated up to 324 ^oC is shown in (b).

The second reaction displayed in Fig. 5(a), which took place at a rather high temperature of about 440 ºC (peak temperature), is an exothermic reaction and refers to a big cube→fcc phase transformation, as was suggested by El-Eskandarany and Inoue [9].

In order to understand the catalytic effect of big-cube phase on improving the hydrogenation/dehydrogenation properties of nanocomposite MgH_2, the absorption (Fig. 7(a)) and desorption (Fig. 7(b)) kinetics achieved at 250 °C were investigated. The sample absorbed about 4.7 wt.% H_2 within 80 s and reached to saturated at about 4.9 wt.% H_2 after 92 s, as displayed in Fig. 7(a). Then, the nanocomposite powders desorbed about 4 wt.% H_2 within 150 s and completely released about 4.9 wt.% H_2 after 320 s (Fig. 7(b)). Comparing these results with those obtained for pure MgH_2 system (see for example [3]) one can conclude that the synthesized nanocomposite MgH_2/10 big-cube Zr_2Ni system enjoys fast absorption and desorption kinetics, suggested by the superior role of big-cube nanocatalysts on improving the hydrogenation/ dehydrogenation behavior of MgH_2 system.

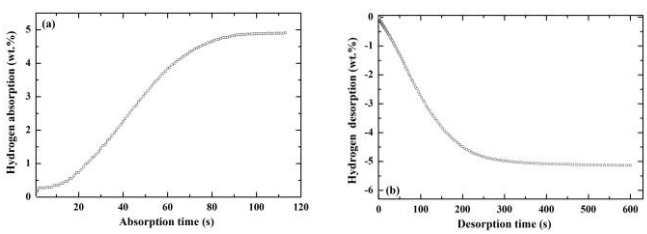

Figure 7: (a) absorption and (b) desorption kinetics developed at 250ºC for MgH_2 powders doped with big cube Zr_2Ni and then ball milled for 50 h.

The hydrogen chargeability and cyclic stability of nanocomposite MgH_2/10big-cube Zr_2Ni system, was carried out at 250ºC. Figure 8 displays the cyclic-life-time curves of the examined nanocomposite powders prepared in the present study. The powders possessed extraordinary high absorption/desorption cycles (2546 complete cycles) covered within 1240 h, as elucidated in Fig. 8. No remarkable degradation in the hydrogen storage capacity could be observed during the first 250 h where the sample maintained its hydrogen chargeability at a constant value of 5 wt.%. A slight monotonical decreasing in the hydrogen storage capacity (about 0.5 wt.%) can be seen when the sample was subjected to further cycle-life-time (above 250 h). This slight degradation occurred due to the agglomeration of the powder particles and the grain growth happened in the big-cube and Mg grains, as was checked by SEM and TEM analysis (not shown here).

4 CONCLUSIONS

Reactive ball milling technique was employed to fabricate nanocrystalline MgH_2 powders, using high energy

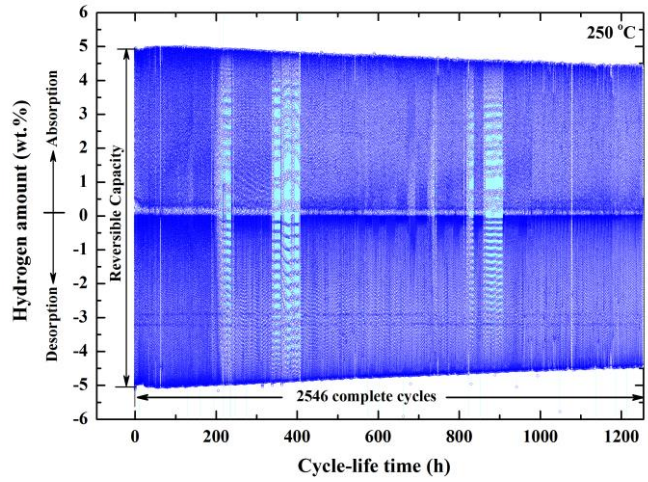

Figure 7: (a) absorption and (b) desorption kinetics measured at 250ºC for for MgH_2 powders doped with big cube Zr_2Ni and then ball milled for 50 h.

ball milling technique. The synthesized powders were mechanically ball milled for 50 h together with 10 wt.% of synthesized big-cube Zr_2Ni nanocrystalline powders to form uniform nanocomposite powders. This new nanocomposite binary system showed fast hydrogenation and dehydrogenation kinetics at 250ºC. Moreover, the synthesized nanocomposite system possessed extraordinary high absorption/desorption cycles of 2546 cycles with a measured cycle-life-time of 1240.

REFERENCES

[1] M Sherif El-Eskandarany, "Mechanical Alloying for Nanotechnology, Materials Science and Powder Metallurgy," 2nd ed., Elsevier Publishing, Oxford-UK, 2015, in press.

[2] M. Sherif El-Eskandarany, K. Sumiyama, K. Aoki, and K. Suzuki, Mater. Sci. Forum, 88, 801-808, 1992.

[3] M. Sherif El-Eskandarany, Ehab Shaban, and Badryiah Al-Halaili, Int. J. Hydrogen Energy, 39, 12727-12740, 2014.

[4] G. Liang, J. Huot, S. Boily, Neste A. Van and R. Schulz, J. Alloys Compd., 292, 247–452, 1999.

[5] T. Sadhasivama, M. Sterlin Leo Hudson, K. Sunita Pandey, Ashish Bhatnagar, K. Singh Milind, K. Gurunathan, and O.N. Srivastav, J. Hydrogen Energy, 38, 7353-7362, 2013.

[6] J. Huot, D.B. Ravnsbæk, J. Zhang, F. Cuevas, M. Latroche, T.R. Jensen, Prog Mater Sci, 58, 30-75, 2013.

[7] M. Sherif El-Eskandarany, Intermetallics, 61, 2015, in press.

[8] Z. Altounian, E. Batalla, J.O. Strom-Olsen, and W.L. J. Walter, J. Appl. Phys., 61, 149-154, 1987.

[9] M. Sherif El-Eskandarany, A. Inoue, Physical Review B, 75, 224109 – 1 to 224109-9, 2007.